Supramolecular Chemistry

DOI: 10.1002/ange.201304887

$\{Mo_{24}Fe_{12}\}$ Macrocycles: Anion Templation with Large Polyoxometalate Guests**

Xikui Fang, Laura Hansen, Fadi Haso, Panchao Yin, Abhishek Pandey, Larry Engelhardt, Igor Slowing, Tao Li, Tianbo Liu, Marshall Luban, and David C. Johnston*

Anion templation has emerged as a valuable tool for constructing a wide variety of inorganic[1] and organic[2] supramolecular assemblies. Inspired by nature's ability to selectively bind and transport anionic species, which constitute about two-thirds of all substrates and cofactors in biological processes,[3] chemists have developed artificial receptors in the form of macrocycles, cages, and interlocked structures that are capable of hosting and detecting small guest anions (e.g. ClO_4^-, SO_4^{2-}, and halides).[4] Hawthorne's [12]mercuracarborand-4[5] and Lehn's circular helicates[6] in the 1990s are notable early examples.

Herein, however, we want to bring attention to non-covalent templation utilizing polyoxometalates (POMs),[7] a group of anionic clusters that are significantly larger and structurally more complex. The assembly of giant polyoxomolybdate "wheels" by Müller and co-workers, for example, is believed to be mediated by sizable polyanion species,[8] some of which are in transient existence but can be observed with the aid of a flow reactor designed by Cronin et al.[9] More recent progress in the syntheses of high-nuclearity silver alkynyl clusters, led by Mak, Wang, and others,[10] is another elegant example of templation exploiting in-situ-generated POM guests, which are bound primarily by electrostatic attraction and symmetry matching. We describe herein the template-directed formation of macrocycles based upon two of the classical POMs, Keggin-[11] and Dawson-type[12] anions, driven instead by hydrogen bonding. These unique supramolecular assemblies clearly illustrate the power of hydrogen bonds—individually weak yet collectively strong.

Before delving into the pictorial structural chemistry of these assemblies, we provide a brief summary of the chain of events that led to their discovery. Initially, the host–guest complex $[(SiMo_{12}O_{40})\subset Mo_{24}(Fe\text{-}edta)_{12}O_{72}]^{16-}$ (**1**) was isolated as a Na^+ salt from the one-pot reaction of sodium molybdate, iron(III) chloride, ethylenediaminetetraacetate (edta), and the Keggin anion $[SiMo_{12}O_{40}]^{4-}$ ($\{SiMo_{12}\}$) under acidic conditions ($pH \approx 2$), which produced diamond-shaped yellow crystals. These crystals were exceptionally fragile and soft, characteristics typically seen for loosely packed crystals of biological macromolecules. They also produced a very weak X-ray diffraction pattern (up to 2.8 Å resolution), again indicative of weak intermolecular contacts and/or high solvent contents. A better data set (resolution to ca. 1.5 Å) was later obtained using a high-intensity synchrotron X-ray source at the Advanced Photon Source of Argonne National Laboratory. The data, suggesting a cubic cell ($Fd\bar{3}$, $V_{cell} = 224271$ Å^3 with $Z = 16$ formula units per unit cell), did establish a cyclic profile of the structure, but many atoms on and inside the ring could not be located because of the resolution limit.

When triethanolammonium ($TEAH^+$) was subsequently introduced as the counter cation in the above reaction, it produced prismatic crystals of **1**. The new crystals, to our surprise, greatly extended the diffraction resolution to approximately 1.2 Å using only an in-house X-ray source. Presumably this improvement is because the long-arm hydroxy groups on $TEAH^+$, whose presence was confirmed by IR and elemental analyses but could not be located in difference Fourier maps owing to disorder, have facilitated stronger intermolecular contacts, hence tighter packing and better ordering of molecules within the crystal lattice. Additional enhancement in diffraction power (resolution under 0.95 Å) was achieved when the crystals were subjected to post-crystallization dehydration by slowly evaporating the mother liquor containing the crystals, a step that gradually increased salt concentration and further reduced the amount of disordered solvent between molecules. The $TEAH^+$ crystals of **1**, of the formula $(TEAH)_6H_{10}$-**1**$\cdot 129H_2O$ (**1a**), turn out to be in a monoclinic cell ($P2_1/c$, $V_{cell} = 22762$ Å^3 with $Z = 2$).[13] Despite introduction of the bulky $TEAH^+$ counterions, the amount of space occupied by each molecule shrinks by 18.8%, compared with that of the cubic crystal of the Na^+ salt, from 14017 to 11381 Å^3. This translates into a more than

[*] Dr. X. Fang, L. Hansen, Dr. A. Pandey, Dr. I. Slowing, Prof. Dr. M. Luban, Prof. Dr. D. C. Johnston
US DOE Ames Laboratory and Department of Physics and Astronomy, Iowa State University
Ames, IA 50011 (USA)
E-mail: xfang@ameslab.gov
F. Haso, Dr. P. Yin, Prof. Dr. T. Liu
Department of Polymer Science, University of Akron
Akron, OH 44325 (USA)
Prof. Dr. L. Engelhardt
Department of Physics and Astronomy, Francis Marion University
Florence, SC 29502 (USA)
Dr. T. Li
X-ray Science Division, Advanced Photon Source, Argonne National Laboratory, Argonne, IL 60439 (USA)

[**] Ames Laboratory is operated for the U.S. Department of Energy (DOE) by Iowa State University under Contract No. DE-AC02-07CH11358. T.L. acknowledges support from the NSF (CHE-1026505). The Advanced Photon Source, an Office of Science User Facility operated for DOE Office of Science by Argonne National Laboratory, is supported by the U.S. DOE under Contract No. DE-AC02-06CH11357. We are grateful to Dr. Gordon Miller for granting access to X-ray facilities and Dr. Chih-Chia Su for assistance with synchrotron X-ray measurements.

Supporting information for this article is available on the WWW under http://dx.doi.org/10.1002/anie.201304887.

30% reduction in solvent content (estimated using the SQUEEZE[14] routine of PLATON[15] software) and accounts for the remarkable improvement in diffraction quality, thereby allowing for a complete structure solution of the host–guest assembly and a detailed analysis of the supramolecular interactions therein. The resulting structure is shown in Figure 1 a,b.

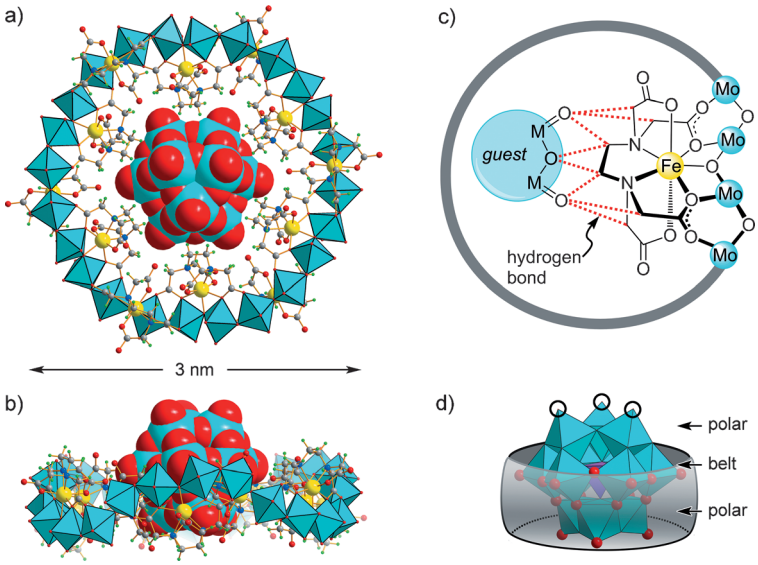

Figure 1. a) Axial view and b) side view of the X-ray crystal structure of **1** in **1a**. Fe yellow, Mo turquoise, Si purple, O red, C gray, N blue, H green. c) Sampling of hydrogen bonds between the Keggin guest and an edta ligand on the host molecule. The red dotted lines represent hydrogen bonds. d) The embedded guest $\{SiMo_{12}\}$ utilizes surface oxygen atoms (red spheres) of both a polar layer and a belt layer to achieve optimal hydrogen binding to the host (in gray). Black circles indicate terminal oxygen atoms that are not properly aligned for hydrogen bonding.

The host molecule is centrosymmetric, made up of a ring of 24 corner-sharing MoO_6 octahedra with 12 appended Fe-edta groups. The Mo_{24} ring is wavy rather than flat (Figure 1 b) owing to constraints imposed by the Fe-edta units, six of which project inwardly toward the core and the remaining six reside on the rim of the macrocycle, giving rise to a non-crystallographic S_6 symmetry for the host. Each edta ligand, aside from chelating one Fe center, utilizes two glycine arms to bridge four adjacent Mo sites of the Mo_{24} ring. All Fe centers are seven-coordinate and feature a pentagonal bipyramidal geometry, as found earlier in many discrete Fe^{III} edta complexes.[16] Bond valence sum (BVS) calculations also indicate the Fe centers are all in the +3 oxidation state (BVS 2.92–3.02).[17]

The templating Keggin anion fits tightly into the cavity of the host; its size and shape complementarity is evident from the X-ray structure. The crystallographic inversion center at the middle of the macrocyclic host results in the encapsulated Keggin cluster being disordered over two equally weighted sites. For clarity, only one position of the guest is shown in Figure 1. The key feature is that the embedded guest is not placed concentrically with the host. The central Si atom of the Keggin anion is perched 2.51 Å above the equatorial plane of the host (defined roughly by the six inner Fe centers). This also raises the important question about host–guest interactions.

The macrocycle itself, $[Mo_{24}\{Fe(edta)\}_{12}O_{72}]^{12-}$, is highly negatively charged, and therefore inclusion of an anionic guest is seemingly counterintuitive given Coulombic repulsion. More surprisingly, an electrostatic potential map (see the Supporting Information) of the host molecule indicates that its central pocket is the most negative region, hardly a propitious environment for anionic species. For the host–guest complex to form and stabilize, attractive interactions thus have to be present and strong enough to more than compensate for the repulsive electrostatic forces.

That attractive driving force is found to be hydrogen bonding. Figure 1 c sketches part of the complex network of hydrogen bonds that knit together the host–guest pair in **1**. Exterior oxygen atoms of the Keggin guest, terminal and bridging ones, are the recipients of hydrogen bonds originating from CH_2 groups of the inward-pointing edta ligands. All hydrogen bonding interactions are fairly weak, as expected from C–H donors, with donor(C)–acceptor(O) distances longer than 3.2 Å.[18] In total, there are dozens of hydrogen bonds involved, but the number cannot be precisely determined given that the C···O distances and C–H···O angles are broadly distributed and it is not possible to choose a strict cutoff.

Despite being individually weak, these hydrogen bonds collectively drive and stabilize this giant assembly. To do so, the host and guest components are suitably positioned so as to achieve maximum interactions. Figure 1 d shows only the oxygen acceptors on the Keggin guest. The fact that the guest anion is not placed centrally within the macrocycle enables the host to be in immediate contact with both a belt layer and a polar layer (i.e. a $\{SiMo_9\}$ moiety) of the Keggin framework, not just the belt layer itself should it be otherwise. It must also be noted that there is a subtle structural difference between the top and the bottom triads of MoO_6 octahedra, which are corner-shared and edge-shared, respectively. As a consequence, the three terminal oxygen atoms (circled in Figure 1 d) on the top layer are too vertically tilted to support effective hydrogen bonding with edta donor groups that approach horizontally. This configurational difference thus explains the host's preference for the bottom two layers, as opposed to the top two layers, for encapsulation. In short, both the position and orientation of the embedded guest are dictated by its tendency to maximize hydrogen bonding capacity.

In search of different templates, and to further illustrate the driving force of templation, we also looked into a number of other POMs of various size and shape, in the hope that smaller or larger macrocycles might be generated. However, of the many polyanions we attempted, only the Dawson-type[12] $[P_2W_{18}O_{62}]^{6-}$ ($\{P_2W_{18}\}$) succeeded, yet again affording the $\{Mo_{24}Fe_{12}\}$ macrocycle. X-ray crystal structure analysis[13] of the new complex $[(P_2W_{18}O_{62})\subset Mo_{24}(Fe\text{-}edta)_{12}O_{72}]^{18-}$ (**2**)

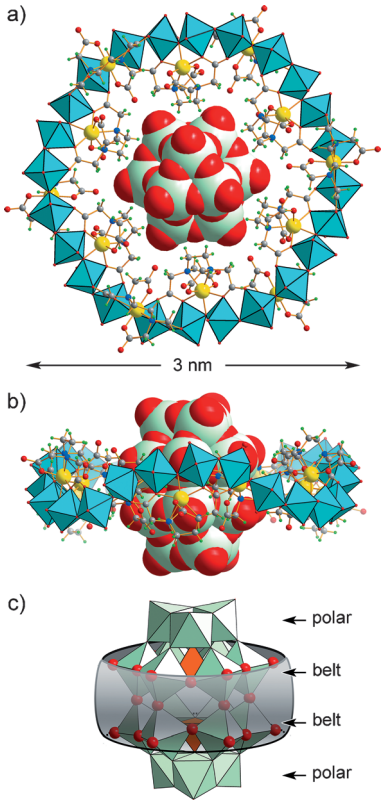

Figure 2. a) Axial view and b) side view of the X-ray crystal structure of **2** in **2a**. c) Inclusion of the Dawson guest $\{P_2W_{18}\}$ in the macrocycle, with surface oxygen acceptors highlighted. Colors same as **1**, except for W light green and P orange.

was also performed on a $TEAH^+$ salt, $(TEAH)_7K_2H_9$-**2**·$116H_2O$ (**2a**).

Although of larger size and elliptical shape, the Dawson anion is a close relative of the Keggin species with a similar transverse profile that matches the sixfold improper rotation symmetry of the macrocycle (Figure 2a). It may therefore be concluded that it is not the overall size or geometry of the guest that matters; templation depends rather on the very portion of the guest structure that initiates the binding. The charge of the anion guest appears to have little influence on the structure formed, as the $\{Mo_{24}Fe_{12}\}$ macrocycle is obtained with both −4 (Keggin) and −6 (Dawson) charged species.

The most revealing feature of complex **2** is the location of the Dawson guest inside the macrocycle. The guest can be formally regarded as two $\{PW_9\}$ subunits fused together. But instead of accommodating a $\{PW_9\}$ moiety (i.e. one belt layer and one polar layer) as in **1**, the host now encircles the two equatorial belts so that the guest is locked right at the center of the cavity (Figure 2c). This arrangement is because a belt layer has more oxygen acceptors than a polar layer, particularly terminal ones that are easily accessible to donor groups. Hydrogen-bonding interactions occurring at belt layers of the guest are thus more robust, imparting additional stability to the host–guest assembly. Once again, hydrogen bonding is the key and it determines how the Dawson guest is positioned in the host cavity.

In the crystal structures of both complexes, the Fe···Fe distances alternate between 6.0 and 6.4 Å along the macrocycles. Although these distances are comparable to those seen for the renowned Keplerate $\{Fe_{30}M_{72}\}$ clusters,[19] the exchange interactions in **1a** and **2a** are at least an order of magnitude weaker, based on the magnetic measurements. For both compounds, the magnetic susceptibility χ was measured in the temperature range from 2 to 300 K at a magnetic field $H = 0.1$ T (Figure 3). For $T > 100$ K, $\chi T \approx 53$ $cm^3\,K\,mol^{-1}$,

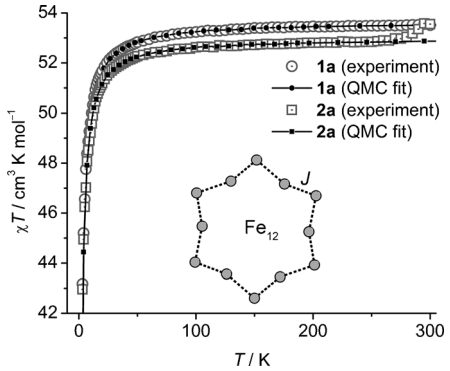

Figure 3. Temperature dependence of χT for **1a** and **2a** at 0.1 T and QMC fitting results obtained by adopting a 1-J model for the Fe_{12} rings (inset).

which corresponds to the Curie constant for 12 Fe^{III} ions ($C = 0.125\,cm^3\,K\,mol^{-1} \times N \times g^2 \times s(s+1) \approx 52.5\,cm^3\,K\,mol^{-1}$ for $N = 12$, spin $s = 5/2$, and spectroscopic splitting factor $g \approx 2$). As adopting a 2-J model did not lead to noticeable improvement in fitting versus a 1-J model, we modeled both compounds using the following Heisenberg Hamiltonian [Eq. (1)],

$$\hat{H} = J\sum_{n=1}^{12}\vec{s}_n \cdot \vec{s}_{n+1} + g\mu_B H\sum_{n=1}^{12}s_{nz} \qquad (1)$$

where $\vec{s}_{13} \equiv \vec{s}_1$, J is the exchange constant (antiferromagnetic for $J > 0$), and $\vec{s}_n$ is the quantum operator spin vector for site n. The dimension of the Hilbert space for a system of 12 exchange-coupled spins 5/2 is $6^{12} = 2.18 \times 10^9$, which is beyond the capabilities of matrix diagonalization. Therefore calculations have been performed using a Quantum Monte Carlo (QMC) method with the stochastic series expansion implementation from algorithms and libraries for physics simulations (ALPS).[20] The solid curves in Figure 3 provide the best fit to the experimental data sets. For both compounds, the root-mean-square deviation between the measured and calculated χT data is $0.03\,cm^3\,K\,mol^{-1}$. The best fits are obtained when $J/k_B = 0.13(1)$ K, $g = 2.022(3)$, $\chi_0 = -5.0(0.8) \times 10^{-3}\,cm^3\,mol^{-1}$ for **1a**; $J/k_B = 0.12(1)$ K, $g = 2.009(3)$, $\chi_0 = -6.5(1.0) \times 10^{-3}\,cm^3\,mol^{-1}$ for **2a**. The constant χ_0 is our estimate for the sum of the diamagnetism and temperature-independent paramagnetism, which have been added to the experimental data for the plots in Figure 3. We note that for both **1a** and **2a** a reasonably good fit to these data can be achieved using a model with no coupling ($J = 0$) and adopting a single-ion anisotropy coefficient $D \approx -0.5\,cm^{-1}$ for each

Fe^{III} ion (the minus sign indicates easy-plane anisotropy). This estimate of D is relatively close to values quoted in the literature for other Fe^{III} systems.[21] Magnetization $M(H,T)$ measurements for fixed T at 2 K have also been performed; the data and fitting results are given in the Supporting Information.

Solution studies indicated that both host–guest complexes maintain their solid-state structures in solution, and we found that no free $\{Mo_{24}Fe_{12}\}$ macrocycle could be isolated or detected without an encapsulated guest. In aqueous solution at room temperature, the ^{29}Si and ^{31}P NMR signals for the central atoms of the Keggin and Dawson guests in **1** and **2** are too broad to be observed due to their proximity to multiple paramagnetic Fe^{III} centers, implying that the guests remain entrapped in the cavity. If external guest molecules were added, however, their signals could be detected. When $[P_2W_{18}O_{62}]^{6-}$, for example, was added to a solution of **2** in D_2O, it appeared in ^{31}P NMR at $\delta = -12.4$ ppm as free anions. No exchange with external POM anions was observed, either. Adding an excess amount of $[SiMo_{12}O_{40}]^{4-}$ to a solution of **2** would not replace the encapsulated Dawson anion even at elevated temperature (80 °C), and vise versa for **1**. Additional evidence for their solution stability came from small angle X-ray scattering experiments; the experimental and simulated curves have similar features (see the Supporting Information). On the basis of the above results, it appears the templating POM anions are held so firmly by an array of hydrogen bonds that they become an integral part of the overall structures they assist in forming. Steric effects may play a role, as well. Inspection of space-filling models (see the Supporting Information) indicates that steric hindrance imposed by edta ligands likely prevents the guests from rotating or slipping out of the cavity.

In summary, the ability of large POM anions to act as templating agents has been clearly demonstrated with the formation of $\{Mo_{24}Fe_{12}\}$ macrocycles. This supramolecular templation relies on the concerted action of a multitude of weak hydrogen bonds. It is also remarkable that these hydrogen-bond-templated processes take place in highly competitive aqueous media, whereas most anion templation studies have been carried out, reluctantly perhaps, in aprotic solvents so that hydrogen binding sites are not swamped by water molecules. The results are thus encouraging for the development of anion receptors/sensors in aqueous solutions.

Received: June 6, 2013
Published online: August 13, 2013

Keywords: anion templation · hydrogen bonds · magnetism · polyoxometalates · supramolecular chemistry

[1] L. S. Evans, P. A. Gale, *Dekker Encyclopedia of Nanoscience and Nanotechnology*, *2nd ed.*, Taylor and Francis, New York, **2009**, pp. 178–190.
[2] P. D. Beer, M. R. Sambrook, *Dekker Encyclopedia of Nanoscience and Nanotechnology*, *2nd ed.*, Taylor and Francis, New York, **2009**, pp. 191–202.
[3] J. W. Steed, J. L. Atwood, *Supramolecular Chemistry*, *2nd ed.*, Wiley, Chichester, **2009**, p. 225.
[4] a) J. L. Sessler, P. A. Gale, W.-S. Cho, *Anion Receptor Chemistry*, Royal Society of Chemistry, Cambridge, **2006**; b) G. T. Spence, P. D. Beer, *Acc. Chem. Res.* **2013**, *46*, 571; c) R. Vilar, *Struct. Bonding* **2008**, *129*, 175; d) M. S. Vickers, P. Beer, *Chem. Soc. Rev.* **2007**, *36*, 211; e) R. Vilar, *Angew. Chem.* **2003**, *115*, 1498; *Angew. Chem. Int. Ed.* **2003**, *42*, 1460; f) P. D. Beer, P. A. Gale, *Angew. Chem.* **2001**, *113*, 502; *Angew. Chem. Int. Ed.* **2001**, *40*, 486.
[5] Z. Zheng, C. B. Knobler, M. F. Hawthorne, *J. Am. Chem. Soc.* **1995**, *117*, 5105.
[6] a) B. Hasenknopf, J.-M. Lehn, B. O. Kneisel, G. Baum, D. Fenske, *Angew. Chem.* **1996**, *108*, 1987; *Angew. Chem. Int. Ed. Engl.* **1996**, *35*, 1838; b) B. Hasenknopf, J.-M. Lehn, N. Boumediene, A. Dupont-Gervais, A.-V. Dorsselaer, D. Kneisel, *J. Am. Chem. Soc.* **1997**, *119*, 10956.
[7] a) M. T. Pope, *Heteropoly and Isopoly Oxometalates*, Springer, Berlin, **1983**; b) Special Issue on Polyoxometalates (Guest Ed.: C. L. Hill), *Chem. Rev.* **1998**, *98*, 1–389; c) *Polyoxometalate Chemistry*: *From Topology via Self-Assembly to Applications* (Eds.: M. T. Pope, A. Müller), Kluwer, Dordrecht, **2001**; d) A. Proust, R. Thouvenot, P. Gouzerh, *Chem. Commun.* **2008**, 1837; e) A. Dolbecq, E. Dumas, C. R. Mayer, P. Mialane, *Chem. Rev.* **2010**, *110*, 6009; f) Themed issue on Polyoxometalates (Guest Eds.: L. Cronin, A. Müller), *Chem. Soc. Rev.* **2012**, *41*, 7333–7646.
[8] A. Müller, S. Q. N. Shah, H. Bögge, M. Schmidtmann, *Nature* **1999**, *397*, 48.
[9] a) H. N. Miras, G. J. T. Cooper, D.-L. Long, H. Bögge, A. Müller, C. Streb, L. Cronin, *Science* **2010**, *327*, 72; b) H. N. Miras, C. J. Richmond, D.-L. Long, L. Cronin, *J. Am. Chem. Soc.* **2012**, *134*, 3816.
[10] a) G.-G. Gao, P.-S. Cheng, T. C. W. Mak, *J. Am. Chem. Soc.* **2009**, *131*, 18257; b) J. Qiao, K. Shi, Q.-M. Wang, *Angew. Chem.* **2010**, *122*, 1809; *Angew. Chem. Int. Ed.* **2010**, *49*, 1765; c) F. Gruber, M. Jansen, *Angew. Chem.* **2010**, *122*, 5044; *Angew. Chem. Int. Ed.* **2010**, *49*, 4924; d) Y.-P. Xie, T. C. W. Mak, *J. Am. Chem. Soc.* **2011**, *133*, 3760; e) Y.-P. Xie, T. C. W. Mak, *Chem. Commun.* **2012**, *48*, 1123; f) K. Zhou, C. Qin, H.-B. Li, L.-K. Yan, X.-L. Wang, G.-G. Shan, Z.-M. Su, C. Xu, X.-L. Wang, *Chem. Commun.* **2012**, *48*, 5844; g) Y.-Y. Li, F. Gao, J. E. Beves, Y.-Z. Li, J.-L. Zuo, *Chem. Commun.* **2013**, *49*, 3658.
[11] J. F. Keggin, *Nature* **1933**, *131*, 908.
[12] B. Dawson, *Acta Crystallogr.* **1953**, *6*, 113.
[13] Crystal data for **1a** at 173 K: Monoclinic, space group $P2_1/c$, $a = 24.432(2)$ Å, $b = 48.149(4)$ Å, $c = 19.859(2)$ Å, $\beta = 103.012(1)°$, $V = 22762(3)$ Å^3, $Z = 2$. The refinement converged to $R(F_0) = 0.0678$, $wR(F_0^2) = 0.1705$, and GOF = 1.043 for 21482 reflections with $I > 2\sigma(I)$. Crystal data for **2a** at 173 K: Monoclinic, space group $P2_1/c$, $a = 24.390(4)$, $b = 48.786(8)$, $c = 19.907(3)$ Å, $\beta = 101.524(2)°$, $V = 23210(6)$ Å^3, $Z = 2$. The refinement converged to $R(F_0) = 0.0703$, $wR(F_0^2) = 0.1575$, and GOF = 1.048 for 26271 reflections with $I > 2\sigma(I)$. CCDC 941979 and 941980 contain the supplementary crystallographic data for this paper. These data can be obtained free of charge from The Cambridge Crystallographic Data Centre via www.ccdc.cam.ac.uk/data_request/cif.
[14] P. van der Sluis, A. L. Spek, *Acta Crystallogr. Sect. A* **1990**, *46*, 194.
[15] A. L. Spek, *Acta Crystallogr. Sect. D* **2009**, *65*, 148.
[16] a) M. D. Lind, M. J. Hamor, T. A. Hamor, J. L. Hoard, *Inorg. Chem.* **1964**, *3*, 34; b) X. Solans, M. Font-Altaba, J. Garcia-Oricain, *Acta Crystallogr. Sect. C* **1984**, *40*, 635; c) J. M. López-Alcalá, M. C. Puerta-Vizcaíno, F. González-Vílchez, E. N. Duesler, R. E. Tapscott, *Acta Crystallogr. Sect. C* **1984**, *40*, 939; d) R. Meier, F. W. Heinemann, *Inorg. Chim. Acta* **2002**, *337*, 317.
[17] Bond valence sum calculation results. Complex **1**: Fe1 (2.92), Fe2 (2.99), Fe3 (3.02), Fe4 (2.94), Fe5 (2.92), Fe6 (2.99). Complex **2**:

Fe1 (2.91), Fe2 (2.92), Fe3 (2.91), Fe4 (2.88), Fe5 (2.97), Fe6 (2.84).

[18] Weak hydrogen bonds are generally characterized by donor–acceptor distances in the range of 3.2–4.0 Å and bond angles greater than 90°. At the lower energy end, they become hardly distinguishable from van der Waals interactions. See, a) T. Steiner, *Angew. Chem.* **2002**, *114*, 50; *Angew. Chem. Int. Ed.* **2002**, *41*, 48; b) G. A. Jeffrey, *An Introduction to Hydrogen Bonding*, Oxford University Press, Oxford, **1997**.

[19] a) A. Müller, M. Luban, C. Schröder, R. Modler, P. Kögerler, M. Axenovich, J. Schnack, P. C. Canfield, S. Bud′ko, N. Harrison, *ChemPhysChem* **2001**, *2*, 517; b) A. M. Todea, A. Merca, H. Bögge, T. Glaser, J. M. Pigga, M. L. K. Langston, T. Liu, R. Prozorov, M. Luban, C. Schröder, W. H, Casey, A. Müler, *Angew. Chem.* **2010**, *122*, 524; *Angew. Chem. Int. Ed.* **2010**, *49*, 514.

[20] a) B. Bauer, L. D. Carr, H. G. Evertz, A. Feiguin, J. Freire, S. Fuchs, L. Gamper, J. Gukelberger, E. Gull, S. Guertler, A. Hehn, R. Igarashi, S. V. Isakov, D. Koop, P. N. Ma, P. Mates, H. Matsuo, O. Parcollet, G. Pawlowski, J. D. Picon, L. Pollet, E. Santos, V. W. Scarola, U. Schollwoeck, C. Silva, B. Surer, S. Todo, S. Trebst, M. Troyer, M. L. Wall, P. Werner, S. Wessel, *J. Stat. Mech.: Theory Exp.* **2011**, P05001; b) A. F. Albuquerque, F. Alet, P. Corboz, P. Dayal, A. Feiguin, S. Fuchs, L. Gamper, E. Gull, S. Guertler, A. Honecker, R. Igarashi, M. Koerner, A. Kozhevnikov, A. Laeuchli, S. R. Manmana, M. Matsumoto, I. P. McCulloch, F. Michel, R. M. Noack, G. Pawlowski, L. Pollet, T. Pruschke, U. Schollwoeck, S. Todo, S. Trebst, T. Troyer, P. Werner, S. Wessel, *J. Magn. Magn. Mater.* **2007**, *310*, 1187.

[21] A. L. Barra, A. Caneschi, A. Cornia, F. Fabrizi de Biani, D. Gatteschi, C. Sangregorio, R. Sessoli, L. Sorace, *J. Am. Chem. Soc.* **1999**, *121*, 5302.

